A novel Cryo-reduction method to investigate the molecular mechanism of nitric oxide synthases.

Running title: cryo-reduction of native iNOSoxy and bsNOS in the presence of cofactor and dioxygen.

Sophie Bernad[§‖], Albane Brunel[†‖], Pierre Dorlet[†], Cécile Roselli-Sicard[*§] and Jérôme Santolini[†*]

‖ Both authors contributed equally to this work

§ Laboratoire de Chimie Physique, CNRS UMR 8000, Univ Paris-Sud, 91405 Orsay Cedex

[†] CNRS, Laboratoire Stress Oxydant et Détoxication, UMR8221, 91191 Gif-sur-Yvette, France and CEA, iBiTec-S, SB2SM, 91191 Gif-sur-Yvette, France

* To whom correspondence should be addressed:

Jérôme Santolini, CEA-Saclay, iBiTec-S, SB2SM, 91191 Gif-sur-Yvette, France

Tél: (33) 1 69 08 53 63

Fax: (33) 1 69 08 87 17

jerome.santolini@cea.fr

Cécile Roselli-Sicard, Univ Paris-Sud, Laboratoire de Chimie Physique, CNRS UMR 8000, Bâtiment 350, 91405 Orsay Cedex

Tél: (33) 1 69 15 77 32

Fax: (33) 1 69 15 61 88

cecile.sicard@u-psud.fr

Substrate-cofactor	Conditions	υ_5	υ_7	υ_{16}	υ_4	υ_3	υ_{10}	υ_{4pp}
Substrate and cofactor free	Ferric heme Before irradiation	1129.1	677	753.5	1374.2	1503.3	1627.3	N.D.
	Ferric heme anaerobic irradiation	1130.7	676	751.1	1376	1506.8	N.D.	N.D.
	Ferric heme air-saturated irradiation	1131.9	675	751	1374.8	1502.1	N.D.	N.D.
	Ferrous heme reduced with dithionite	1131.2	674.6	746.7	1348.9 1368.2 1391.9	1467.8	1619.5	1424.8
	Ferrous heme anaerobic irradiation	N.D.	676.4	N.D.	1351.5 1391.2	1471.8	N.D.	1426.2
	Ferrous heme air-saturated irradiation	1127.5	675.2	N.D.	1350.3 1391.2	1470.6	N.D.	1425.1
Arg-H_4B	Ferric heme Before irradiation	1121.6	676.9	753.9	1373.8	1489.3	1627.4	1429.3
	Ferric heme Anaerobic irradiation	1129	674	753	1373.7	1491.6	1627.1	1429.7
	Ferric heme air-saturated irradiation	1119?	675	ND	1372.5	1490.5	1626	ND
	Ferrous heme Reduced with dithionite	1126	671.7	747.6	1349.1 1366.6 1393.5	1469.4	1619	1423.1
	Ferrous heme anaerobic irradiation	1126	674	747.6	1349.1 1392.3	1469.4	1620	1425.1
	Ferrous heme air-saturated irradiation	1127.2	675.2	747.6	1349.1 1391.2	1470.6	1619	1425.1

Table S1. Vibrational modes of the porphyrin of iNOSoxy before and after gamma-irradiation. Comparison between various conditions (anaerobic *vs* air-saturated, in the presence or absence of saturating concentrations of substrate and cofactor) and with chemically-reduced (with excess dithionite) iNOSoxy. See experimental procedures for experimental details.

Table S2.

		g_1	g_2	g_3
iNOSox	Before irradiation	7.54	4.14	1.82
H_4B-Arg	After 36.2 kGy	7.54	4.14	1.82
bsNOS	Before irradiation	7.59	4.07	1.80
H_4B-Arg	After 76.5 kGy	7.59	4.07	1.80

Table S2. g-values of the 5cHS species of Fe^{III} of iNOS and bsNOS before and after irradiation. EPR X-band spectrum conditions were as follows: microwave frequency, 9.49 GHz; microwave power, 4.0 mW; field modulation amplitude, 1 mT; temperature, 10 K.

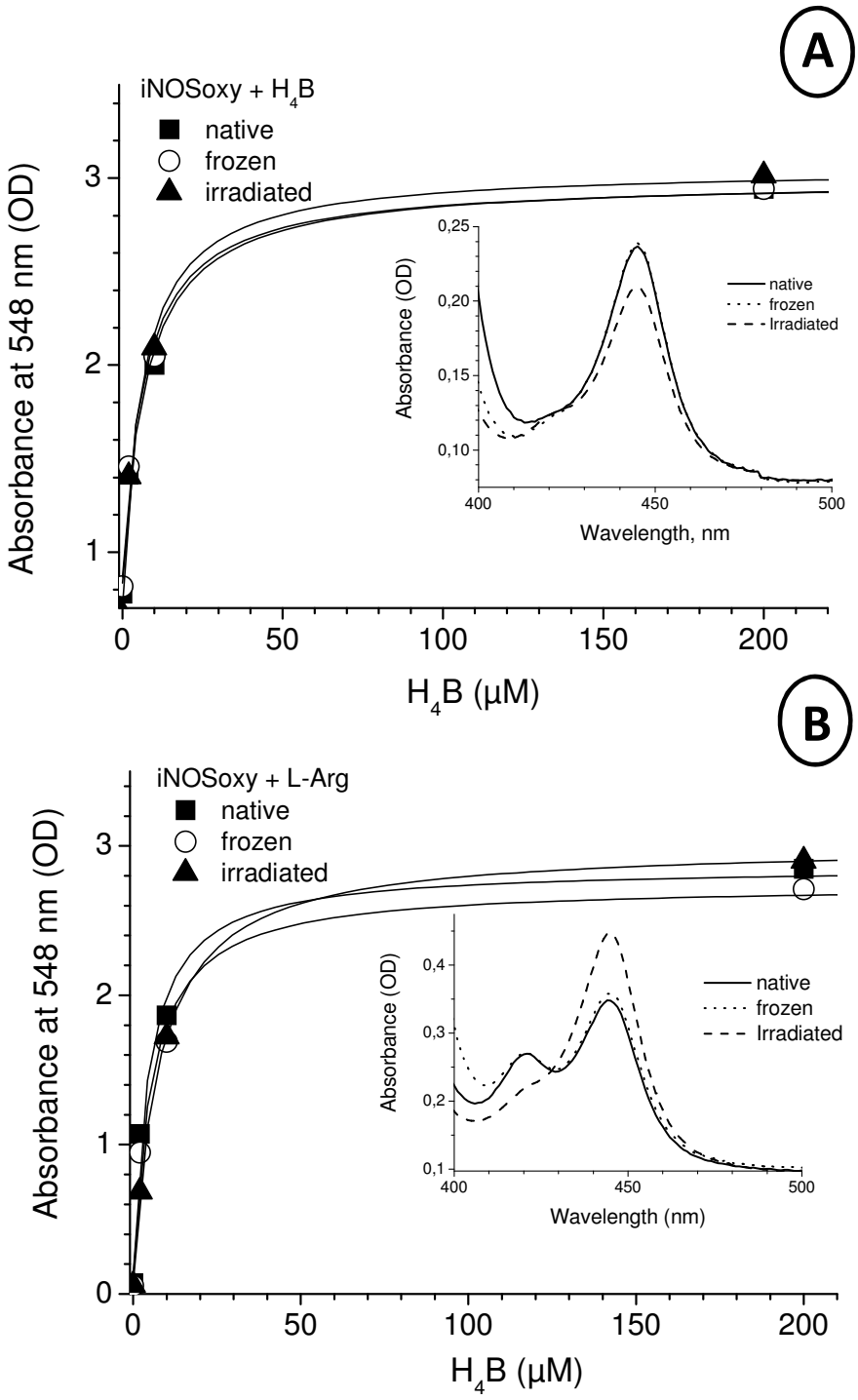

FIGURE S1

Figure S1: Impact of gamma-irradiation on iNOSoxy structure and function. Two samples of 150 µM iNOSoxy were gamma-irradiated with a ^{60}Co source up to 60 kGy in the presence of 800 µM H_4B (Panel A) and in the presence of 5 mM L-Arg (Panel B). The catalytic activity of iNOSoxy from native (full square), frozen (open circle) and irradiated (full triangle) samples were determined by the Griess Assay (Main panels). iNOS samples

were diluted (final concentration 300 nM) in the assay buffer (KPi 0.1 M pH 7.4; Glycerol 10%; DTT 1 mM; BSA 0.1mg/mL; SOD 25 U/mL). After addition of H_4B (between 0.5 and 200 µM final), the samples were incubated 30 minutes at 30°C. Reaction was triggered by the addition of saturating concentrations of NOHA (10 mM final) and H_2O_2 (30 mM). After 10 minutes at 30°C, the reaction was stopped by addition of catalase. Nitrite concentration was measured by addition of Griess reagent and the rate of nitrite production was plotted as a function of H_4B concentration. Simulation to a hyperbolic function gives rise to the V_{max}, V_o and $K_{d,H4B}$ parameters for each condition. The stability of the proximal ligation was investigated for all conditions by determining the P420/P450 transition of the $Fe^{II}CO$ complexes (Inset). iNOS samples were diluted (3-5 µM final concentration) in a KPi 0.1 M pH 7.4, L-Arg 10 mM, H_4B 80 µM buffer. $Fe^{II}CO$ complexes were obtained by addition of dithionite and CO flush. **Panel A.** the nitrite production of iNOSoxy with H_4B was similar for the native, frozen and irradiated samples. V_{max} was respectively 63.6, 61.4, 68.5 s^{-1} and the apparent K_d for H_4B was comparable (4.6, 5.50, 7.6 µM, respectively). These results, in agreement with what is commonly reported in the literature, indicate that neither the H_4B binding properties, nor the ability to activate oxygen, are affected by the freezing and irradiation sequence. The UV-Visible characterization of $Fe^{II}CO$ complexes for these three conditions shows a large majority of hexa-coordinated $Fe^{II}CO$ species. The greater stability of irradiated samples (>95% 6c) versus native and frozen samples (70-80 % 6c) might be due to a longer incubation in the presence of L-Arg, which allowed the completion of the 6cLS to 5cHS conversion of the initial ferric enzyme. **Panel B.** The nitrite productions of iNOSoxy + L-Arg show a similar profile as in Panel A and do not show significant differences between native, frozen and irradiated. The V_{max} values are respectively 50.4, 49.5 and 54.6 s^{-1}. The same observation can also be made for the stability of $Fe^{II}CO$ complexes of iNOSoxy + H_4B samples. The proportions of P420 are more pronounced than in Panel A because the 6cLS→5cHS transition is rapidly completed in the presence of pterin cofactors.